IEEE Access
Multidisciplinary | Rapid Review | Open Access Journal

Received 31 August 2023, accepted 28 September 2023, date of publication 18 October 2023, date of current version 26 October 2023.

Digital Object Identifier 10.1109/ACCESS.2023.3325760

RESEARCH ARTICLE

Conception and Design of WSN Sensor Nodes Based on Machine Learning, Embedded Systems and IoT Approaches for Pollutant Detection in Aquatic Environments

YAN FERREIRA DA SILVA[1], RAIMUNDO CARLOS SILVÉRIO FREIRE[2], (Member, IEEE), AND JOÃO VIANA DA FONSECA NETO[3], (Member, IEEE)

[1]Coordination of Electrical Engineering, Universidade Federal do Maranhão, São Luís 65080-805, Brazil
[2]Department of Electrical Engineering, Federal University of Campina Grande, Campina Grande 58428-830, Brazil
[3]Department of Electrical Engineering (DEE), Universidade Federal do Maranhão, São Luís 65080-805, Brazil

Corresponding author: Yan Ferreira da Silva (yan@nca.ufma.br)

This work was supported in part by the National Agency for Petroleum, Natural Gas and Biofuels (ANP); in part by the Human Resources Training Program for the Oil, Natural Gas and Biofuels Sector (PRH-ANP); in part by the National Council for Scientific and Technological Development (CNPQ); in part by the Maranhão Research Support Fund (FAPEMA) and Higher Education Personnel Improvement Coordination (CAPES); in part by the Support Program for Centers of Excellence (PRONEX), Paraíba State Research Support Foundation (FAPESQ); and in part by INCT of Micro and Nanoelectronic Systems (NAMITEC), Universidade Federal do Maranhão (UFMA), through the Graduate Program in Electrical Engineering (PPGEE).

ABSTRACT To prevent and mitigate the environmental impact of the transportation and extraction of oil and its derivatives, the conception, design, development, and implementation of an embedded system for wireless sensor networks (WSN) is presented is this paper. The proposed embedded system is a static sensor node that detects and classifies pollutants in aquatic environments using machine learning and IoT (Internet of Things) approaches. The article presents the development of the sensor node, which consists of three phases. In the first phase, the conception and modeling of the embedded system are presented, including mathematical modeling of the node, the node's power supply system, WSN communication structure, pollutant detection, and classification via machine learning and IoT. The implementation of the static sensor node is presented in the second phase of the project, which includes functional modeling of the measurement, the architecture of the embedded system, and its physical structure. In the last phase, the detection and classification tests of the proposed sensor node are presented, including implementing five sensors. They are evaluated indoors by analyzing seawater samples with gasoline and diesel, pH and turbidity measurements of seawater and freshwater with gasoline, and experiments through direct and indirect measurements of seawater and diesel. Since the initial results of the indoor experiments are satisfactory, the proposed sensor node is regarding as a promising device for detecting and classifying pollutants in real-world aquatic environments.

INDEX TERMS Embedded systems, IoT, wireless sensor network, high performance computing, machine learning detection, tracking, pollutants in aquatic environments, fuel oil and petroleum products, connectivity, coverage.

I. INTRODUCTION

The relevance of Wireless Sensor Networks (WSN) for monitoring and controlling industrial activities, transportation, agriculture, and aerospace are already ubiquitous in contemporary society. In these networks, sensor nodes play an essential role, that is, they are the main components to perform measurements of certain variables. To contribute for detecting pollutants in aquatic environments, an innovative methods to the design and development of static sensor

The associate editor coordinating the review of this manuscript and approving it for publication was Chin-Feng Lai.

nodes for WSNs is presented in this article. The processing core of the measurements and information collected by the node's sensors are based on theoretical and technological foundations supported by machine learning [12], [22] and embedded systems approaches [20]. Also, a dedicated embedded system for solving the problem of detecting and classifying petroleum product spills in marine environment and distributed signal processing in WSN is presented in this paper. The estimation methods are embedded and evaluated in sensor networks with static nodes for detecting and tracking oil product spills [2] at sea using case studies.

The development of embedded systems for processing and communication is based on high performance architectures [10], such as RISK, and the local and distributed fusion of sensor signals. In order to detect and classify the pollutant, be it seawater or oil-based fuel, the signals measured by the sensors are processed using machine learning techniques [6], [32]. The proposed method is evaluated on fuel oil and petroleum product leaks [30]. Given the approximations of the proposed models and the amount of available data that are crucial for the estimation of the states of a given process, aiming at the detection and tracking of petroleum products [2], the guarantee of convergence, stability, and robustness for machine learning methods is a property of the proposed method.

The motivation for choosing the topic oil spill in aquatic environment is due to its importance for the environment, as can be seen in [9], [16], and [11]. Companies linked to maritime transportation and its complex dynamic characteristics in relation to a concise online tracking, data are exposed in technical reports and scientific article [3]. The estimation and control strategies are fundamental in this process to ensure energy efficiency [1], [15], [31], [14] and safe operation, to achieve the desired properties and to prevent and minimize environmental impacts damage [4].

This paper presents the state-of-the-art in the context of WSN, relating to sensor nodes, embedded systems, IoT and machine learning. The importance of embedded systems lies in their penetration in to most human activities. Moreover, activities increasingly depend on their real-time capabilities, such as sensing, processing, communicating, and acting [17]. Regarding the need to address problems that arise due to the complexity of embedded systems, the authors [22], [24] state that complexity and applications with IoT impose design constraints that demand the development of methods to find the best compromise between the different design objectives of the embedded system. A low-cost sensor node for a WSN is presented in [7], can detect through a sensor array, accelerometers, gyroscopes, Global Positioning System (GPS), and infrared thermal sensors based on oil films that emit heat more slowly than the surrounding water during the day. However, the process is reversed during the night, making it vulnerable to lighting conditions. The captured signals are processed, and their estimated information is transmitted by telemetry, alerting the occurrence of a possible oil spill and informing the location and thickness of the slick. Recently, advances in hardware and software oriented towards AI applications in embedded systems and IoT [20] with limited resources and energy for a wide range of applications have increased the importance of finding effective solutions to the mentioned problems [17], [21].

Because of the importance of embedded systems for operation and their ability to support decision-making, relevant questions, such as security, protection, and reliability are raised, which directly impact physical and data security. Additionally, control, validation, self-testing, and observability of embedded systems in their programmed or acquired operations are significant concerns for their acceptance in critical infrastructures or operations. Furthermore, cost, energy, and maintenance requirements must be considered, given the high number of embedded systems for IoT applications [17], [30]. The cited reference also emphasizes the importance of embedded systems for transferring data for remote processing, fostering a faster real-time response and reducing dependency on data connections. This way, it contributes to improving scalability and increasing security.

Regarding the design of the embedded system, the suggestions and techniques presented in the references that deal with modeling, synthesis, and analysis are considered for the design and implementation of the proposed sensor node. In [10], the authors present modeling, synthesis, and verification for the design of embedded systems. In [18], the authors introduce embedded systems, emphasizing a cyber-physical systems approach. In [20] and [21], the authors present the design of an embedded system, emphasizing embedded systems, cyber-physical systems (CPS) fundamentals, and IoT. In [34], the authors present principles of Embedded Systems Design and distributed computing.

To mitigate the environmental and socio-economic risks caused by oil spills, monitoring the sea using remote sensing plays a crucial role in detecting and combating marine pollution. Fuel spills represent a serious environmental risk, causing significant damage to marine life, coastal ecosystems and fishing resources. In addition, these events have negative socio-economic impacts, affecting the health of coastal communities, the tourism industry, fishing activity and port economic activities. To combat these risks, it is essential to have an efficient, low-cost, real-time monitoring system capable of accurately measuring water quality indicators, combined with machine learning techniques to perform local detection and classification of pollutants spilled by accidents and incidents involving fuels and oil products in coastal environments. To date, existing detection methods have shown limitations in fully meeting these requirements. It is therefore necessary to develop monitoring techniques for detecting pollutants in water.

In view of the problem set out in the previous paragraph, let's establish the problem as follows. Given an aquatic environment with a high level of pollution from the melting of petroleum products, the problem consists of detecting

and classifying the pollutants present in the environment in question. Detection is carried out by a static sensor node of a WSN, which is composed of hardware with four contact sensors on the water surface and communication with a base station to receive the detected signals and the node's estimates. Classification is carried out by an artificial neural network.

The remaining sections of the article discuss the theoretical framework and its associations to enable the proposed method and the performance evaluation results for various pollutant detection scenarios. Section II presents the necessary content for the development of the proposed approach. The topics covered are focused on technology involving concepts related to hardware and the system for capturing and observing the physical phenomenon. The content includes wireless sensor networks, embedded systems, and intelligent sensing. In Section III, the proposed concept and modeling of the embedded system are presented, covering topics related to the problem and general and particular solutions. In Section IV, the process of developing the project and implementing a static sensor node is presented. The results of tests for the sensor node for detecting and classifying pollutants are presented in Section V. The conception and design of sensor nodes to WSN are presented in Section VI.

II. PRELIMINARY

The main concepts of sensor nodes and machine learning, and embedded systems are presented in this section. Specifically, the approaches necessary for developing the design methodology and implementing the embedded system and intelligent framework for identifying and classifying pollutants on the water surface are presented descriptively.

A. WIRELESS SENSOR NETWORK

According to [27], wireless sensor networks are networks of devices with autonomous sensor sets, which may or may not have actuators, where communication is performed through wireless channels, and the spatially distributed sensor nodes to monitor physical or environmental phenomena [23], [27], [28]. The sensor nodes are positioned at certain distances from the phenomenon to be observed, which is not possible with traditional sensor networks. WSNs are used to monitor areas with difficult access or inhospitable, areas such as military confrontation, deserts, volcanoes, dumps, forests and industrial areas [19].

The gathered sensors form a wireless data collection network, locally processing the information and disseminating the resulting data from one point to another. Telecommunication, instrumentation, embedded systems, computer architecture, computational intelligence, and electronics are all study areas directly related to WSNs [33]. WSNs combine sensing technologies, computing (local and distributed processing), and overlay networks to provide computing, storage, networking, sensing, and actuation capabilities (technologies linked to long-distance transmission). These networks are formed by several sensor nodes (static and mobile) communicating with each other and the base station through wireless radio links [19].

B. INTELLIGENT SENSOR NODES AND EMBEDDED SYSTEMS FOR WSN

Embedded systems methods and algorithms for WSN are presented in this section. Smart sensors are devices that perform a series of signal processing operations of the embedded sensor, with the help of microprocessor/microcontroller electronic circuits, using computational resources to perform predefined internal functions, detect parameters, and perform processing and transmission of the acquired signals through communication systems [5], [29].

The sensitivity of the sensors must be planned in terms of long-term measures to increase their lifetime, as technical needs are required to obtain acceptable measurements in harsh environments. Because the sensors are designed to be used for an extended period of time, data collection is continuous and the veracity of the estimated signals, and power consumption must considered. Smart sensors and intelligent sensors meet the requirements for robustness in measurement. The smart Wireless sensor, which is an evolution of the smart sensor, is the most recommended in the sensing application of unhealthy and harsh environments because it has independent processing and wireless signal transmission. They have a significant advantage over traditional wired sensors, which are not a cheap and viable option for this type of application [5].

C. METHODS, ALGORITHMS AND MACHINE LEARNING

The evolution of computing, signals/data processing provided advances in machine learning. Therefore, a new era of opportunities to embed computational intelligence within IoT devices has emerged. Applying low-cost IoT learning techniques, such as microcontrollers to perform tasks such as detection, decision-making, classification, regressions, sensory fusion, among others [25], which are applied in several activities, such as: monitoring of environmental and critical areas, air quality, navigation, energy measurements, wireless sensor networks in an industrial environment for monitoring risk activity. These methods limit the computing device's payload resources and require the deployment of lightweight hardware and inference pipelines. Traditionally, microcontrollers operate with low-dimensional structured sensor signals using classical methods. Significant efforts are being made to embed machine learning algorithms in less complex devices as these methods evolve [25], [26].

III. CONCEPTION AND MODELING OF THE EMBEDDED SYSTEM

The design phase of a sensor node is one of the key points. During this phase, the project specifications in the abstraction phase of the proposed architecture and the components that constitute the node, such as the types of sensors and microcontroller, are presented while observing their consumption and processing power. These specifications directly impact

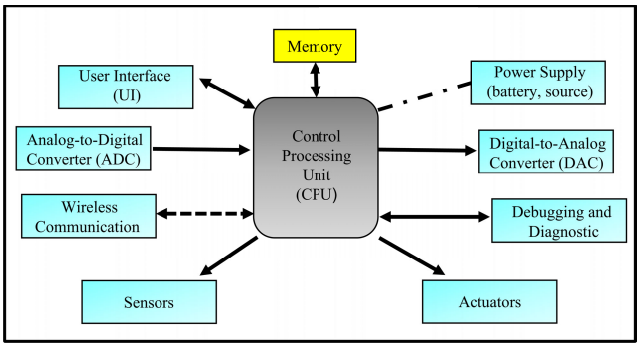

FIGURE 1. Architecture of sensor nodes, peripherals and modules of functional and support systems.

embedded system architecture. Another critical point is the selection of radio technology for transmitting and receiving signals, which directly impacts the size of the board's power supply system, and the appropriate choice ensures a longer life for the sensor node. The block diagram in Figure 1 represents the architecture of the proposed sensor node, highlighting the functional blocks around the processing and control unit (CPU) with the main and auxiliary subsystems of the sensor node, such as: power, computing, interfaces, and communication.

Figure 1 shows the basic architecture of a WSN smart sensor node. In addition to the classic sensor structure, it includes an interface for the actuation system. It is not a passive system that observes its surroundings but is actuated by predefined decisions made during programming or by a remote user.

The design and modeling of the embedded system are discussed in this section, highlighting the composition of the physical layers of the WSN and the architecture of the sensor nodes. However, the main theoretical and technological elements that make up the development of the methodology design and implementation of static sensor nodes are highlighted. The main elements are the mathematical model, node power system, communication structure, and detection and classification via machine learning and IoT. Moreover, each element is presented individually, highlighting the functionality for developing the sensor node.

A. MATHEMATICAL MODELING OF THE NODE

A mathematical model is developed in the physical structure based on set theory for a better understanding. This modeling allows the systematization for theoretical and experimental development of the proposed embedded systems.

Initially, it is established that the node set structure of a WSNs which is given by

$$WSN_{nds} = \{sn_1, sn_2 \ldots sn_i \ldots sn_n\}, \tag{1}$$

where sn_i $(i = 1, \ldots, n)$ is the $i-$th node of the sensor network WSN_{nds} with n nodes. The physical structure of a WSN with n sensor nodes is represented by the set WSN_{nds}.

In terms of physical structure, the $i-$th node of the sensor network with n nodes is formed by a finite set of elements that represent the main and auxiliary functional systems of the architecture of the sensor node in Figure 1. Peripherals, and functional modules is expressed in terms of a set that are connected to the managing element of the services or tasks that are performed to accomplish the goal of the node. Specifically, the nodes are designed to perform the task of detecting and classifying pollutants in the environment.

According to the previous paragraph, the abstraction of the physical structure of the $i-$th node of the WSN_{nds} network with n nodes that represents the architecture of the sensor node in Figure 1 is given by

$$sn_i = \{sp_1, sp_2, \ldots, sp_j, \ldots, sp_k\}, \tag{2}$$

where sp_j represents the $j-$th group of the $i-$th node (sn_i) of the WSN_{nds} network with k groups. Moreover, each group has different characteristics or functionalities representing the architecture, as shown in Figure 1.

For the element sp_j of the group, the elements of the $j-$th group are formed by the finite set which is given by

$$sp_j = \{sp_{j_1} sp_{j_2} \ldots sp_{j_m} \ldots sp_{j_p}\}, \tag{3}$$

where sp_{j_m} is the $m-$th element of the group j with p elements.

In a unified way, the relationships between sets (1), (2), and (3) are summarized in terms of set operations. The new representation of the physical structure of the sensor network and its nodes is given by

$$WSN_{nds} = \left\{ \cup_{j=1,m=1}^{k,p} sp_{j_m} \subseteq_{i=1}^{n} sn_i \right\}. \tag{4}$$

The mathematical model represented by set (4) establishes the complete structural basis of a sensor network with the architecture given in Figure 1. In contrast to the relations (2) and (3), which provide detailed representations of the groups and their set elements, WSN_{nds} represented by (1).

The outputs resulting from the estimates and tasks performed by the sensor network nodes are mappings of information from sets (1), (2), and (3) that are synthesized by the set (4). Consequently, the output of the $i-$th sensor node of the network is given by

$$\hat{y}_q(sp_{j_m}) = f_{nds}\left(\cup_{j=1,m=1}^{k,p} sp_{j_m} \right), \tag{5}$$

where $\hat{y}_q(sp_{j_m})$ is the $q-$th estimated or filtered output of sensor node sn_i of network WSN_{nds} with n nodes.

B. SENSOR NODE POWER SUPPLY SYSTEM

The block diagram in Figure 2 represents the power supply of the logic operation of the sensor node in the network. The power supply system is composed of three main parts that function independently of the central control unit of the embedded system shown in Figure 2, and namely: (1) mini photovoltaic cells, (2) battery charge/discharge controller with embedded system power supply control, and (3) a pack with two 3.7 V- 1400 mAh Li-Po (Lithium Polymer) batteries. The central processing part is represented by (4), the sensing

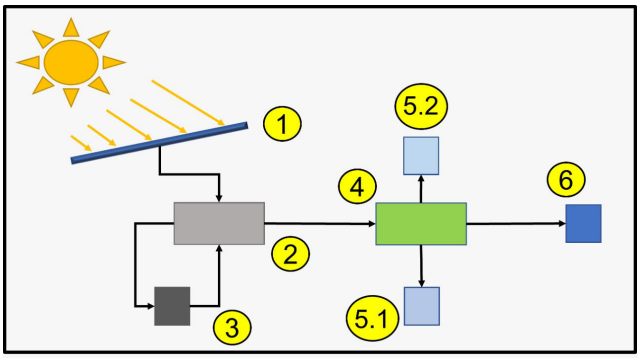

FIGURE 2. Sensor node power supply organization block.

part (5) with its subdivisions: (5.1) liquid contact sensors and (5.2) internal sensing. The signal transmission part is represented by (6), which is the final transmission stage.

Mini photovoltaic cells are used in the battery power system to utilize the sun's energy. It also considers the difficult access to the hardware after installation, which makes maintaining the sensor nodes difficult. A power supply system was designed for the longevity of the system, with mini cells that operate during the day supply energy. The battery pack is recharged in parallel (working only to compensate for interruptions in the supply), and in the absence of the sun, the use of the batteries is 100%, as shown in Figure 2. It has a microcontroller structure (ATtiny85) responsible for controlling the loads and power supply of the embedded system, together with the counter unit with voltage/current sensor, load sensor, voltage converters, and the control unit of the power supply system, and as an under-actuated system that has direct communication with the central control unit of the embedded system (ESP32).

C. WSN COMMUNICATION FRAMEWORK

The communication structure of a WSN and an intelligent sensor node is important to ensure stable communication, and the transmission of observed and estimated signals/data to the destination. The block diagram in Figure 3 represents the WSN communication structure and its stages. The communication mesh has three stages. The final step is that the pre-processed signals/data from the sensor node are accessible to users via a processing software, database, or end-user human-machine interface.

As shown in Figure 3, the communication flow starts in step (1), which is the sensor node, where the microcontroller reads and processes the first measurement signals from the sensors. The flow of the measurement signals is preprocessed in the control unit, and other variables are estimated and compressed following the wireless communication module (in the case of implementation are used LoRa 433 MHz and 5 GHz Wi-fi module embedded in the microcontroller itself). The communication from the sensor node to the base uses a long-distance radio frequency protocol (LoRaWAN) for direct connection to the base station/gateway (2). The signals/data are compressed and sent to the cloud (3) via

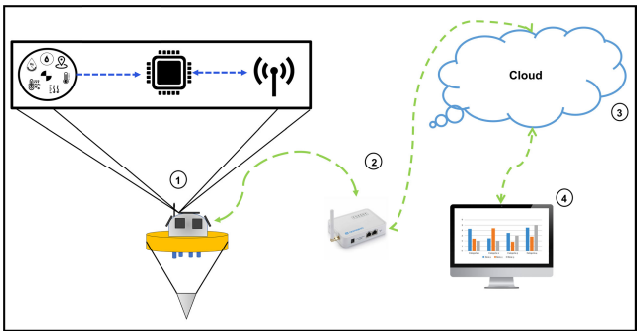

FIGURE 3. The communication system of the sensor node and the stages of the communication flow are: (1) static sensor node, (2) gateway base station, (3) signals stored in the cloud, (4) final destination of measurements and estimates.

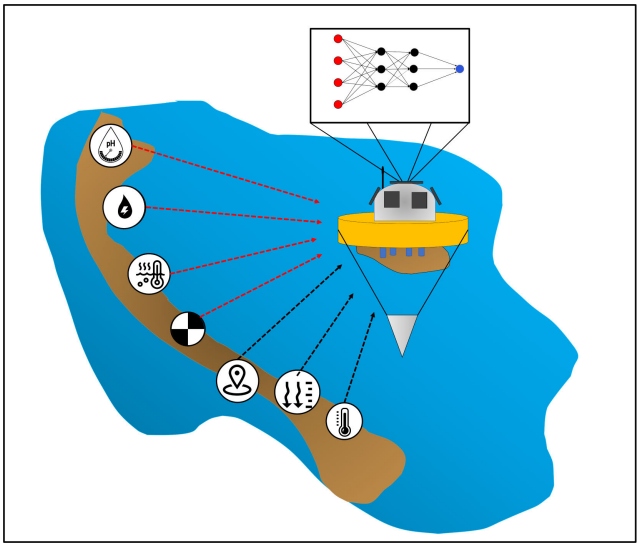

FIGURE 4. Detection, classification and artificial neural network of WSN static nodes.

the message queuing telemetry transport (MQTT) protocol. The gateway with the server/cloud, where the estimated signals/data are stored, enables the final destination (4), data access, and real-time monitoring of a given perimeter via measurements and estimation of the quantities involved.

D. DETECTION AND CLASSIFICATION VIA MACHINE LEARNING AND IOT

The use of signal processing techniques and machine learning for classification, fusion, and state estimation distinguishes intelligent sensor nodes from smart sensors. These approaches enable a wide range of applications and new possibilities for integration with other techniques, such as IoT. Thus, new challenges or frontiers for developing theory, algorithms, hardware, and applications of machine learning methodology and embedded systems are observed.

The association of devices with the operation for detection and classification of the sensor node in a WSN is presented in Figure 4, highlighting the ANN that performs the tasks of detecting and processing signals locally from the node's sensors.

The measurement structure is based on the main states to be observed, which are pH, turbidity, water temperature, and electrical conductivity indices. In the initial tests, the conductivity sensor is not used in conjunction with all the sensors, and these measurement signals are fundamental for the initial analysis of the environment.

Figure 4 shows the observed variables, with the main states to be observed connected in red as input to the multilayer perceptron (MLP) type ANN. The neural network can classify whether the present compound is gasoline or diesel oil based on measurements of pH, liquid temperature (compared to the environment), turbidity, and conductivity. The neural network consists of an MLP with 4 layers, including an input layer and 2 hidden layers with 3 neurons each and one in the output, which is the classifier. TensorFlowLite and the TinyML API are used for supervised training, and the developed algorithms are programmed in Micropython.

IV. DESIGN AND IMPLEMENTATION OF STATIC SENSOR NODES

The core of the proposed methodology for designing and implementing static sensor nodes is presented in this section. The modeling of the embedded system for a sensor node from Section III is applied in developing the proposed methodology. The design of the sensor node with its measurement structure and the construction of the sensor node are also presented.

For the design of the sensor node with its measurement structure and the construction of the sensor node, the choice of sensors is based on Brazilian Standard CONAMA 357/05, which "Provides for the classification of water bodies and environmental guidelines for their framing, as well as establishes the conditions and standards for the discharge of effluents", and on IQA (WATER QUALITY INDEX - National Sanitation Foundation).

A. FUNCTIONAL MEASUREMENT MODELING

The modeling of the measurement structure is based on sets (2) and (3). For the development of the proposed embedded system, and the application presented in this article, the physical structure of the sensor node is represented by

$$sn = \left\{sp_{C_1}, sp_{C_2}, sp_{C_3}, sp_{in_1}, sp_{in_2}\right\}. \tag{6}$$

The internal sensors are divided into k groups. For example, each node can be divided into two groups of sensors sp_C (sensors in contact with liquids) and sp_{in} sensors inside the node.

The generalization of the physical structure of the sensor network is given by

$$WSN_{nds} = \{sp_C \cup sp_{in} \subseteq sn\}. \tag{7}$$

The specific mathematical model for the embedded system of the sensor node is represented by Equation (7), establishing the structural basis of the sensing elements of each node, forming the measurement structure of the WSN that is part of a detection, processing, and signal transmission system of the WSN_{nds}.

Customizing set relations (6) for measurement structure, and the proposed node structure is given by

$$sp_c\phi_c = \left\{Temp_{Liq}, Cond_{Liq}, pH_{Liq}, Turb_{Liq}\right\}, \tag{8}$$

In set (8), $sp_{in}\phi_{in}$ represents the state variables observed through direct and indirect measurements, where the observed variables are of the sensor type sp_C liquid temperature ($TempLiq$), the electrical conductivity of the liquid ($Cond_{Liq}$), hydrogen potential of the liquid (pH_{Liq}), and turbidity ($Turb_{Liq}$). The representation of the sensor groups is given by

$$sp_{in}\phi_{in} = \{Pres_{Env}, Temp_{Env}, Lat_{in}, Long_{in}\}, \tag{9}$$

where the state variables are relative pressure of the environment ($Pres_{Env}$), temperature of the internal environment of the sensor ($Temp_{Env}$) and latitude coordinates (Lat_{in}) and longitude ($Long_{in}$). In set (9), this set of states is generated by the sensor sets $sp_{in}\phi_{in}$.

According to (5), combining the measurements performed by the sensor node (8), and machine learning techniques, the result is the estimation of new states presented by the mapping that is given by

$$\hat{y}(sp_c\phi_c) = \{gas, dieselfuel, polluting\}. \tag{10}$$

The set $y(sp_c\phi_c)$ presents the results, and they are the observed and classified states/identification of the pollutants. In this way, it can detect the presence of gasoline, diesel oil, or other unlisted environmental pollutants (foreign bodies).

B. EMBEDDED SYSTEM ARCHITECTURE

The methodology for developing the hardware of the smart sensor node is based on the functional model of the sensor node, presented in Section III and the IEEE 1451.2 standard. Figure 5 presents the architecture of the embedded system, highlighting the components of its physical structure, such as the power supply system, WSN communication, and sensors. The embedded system manages the water contact sensors, which are used to measure the liquid temperature, water hydrogen ion potential (pH), and turbidity, allowing detection and classification of the compound present in the aquatic environment.

The proposed sensor node architecture in Figure 5 is divided into three blocks, including a signal acquisition block for contact sensors with liquids, a power and load control block (responsible for the energy management of the system), and the main block where the processing elements and connection interface for signal transmission are grouped.

Figure 5 is divided into two parts, with the dashed lines representing the logical part and the solid lines corresponding

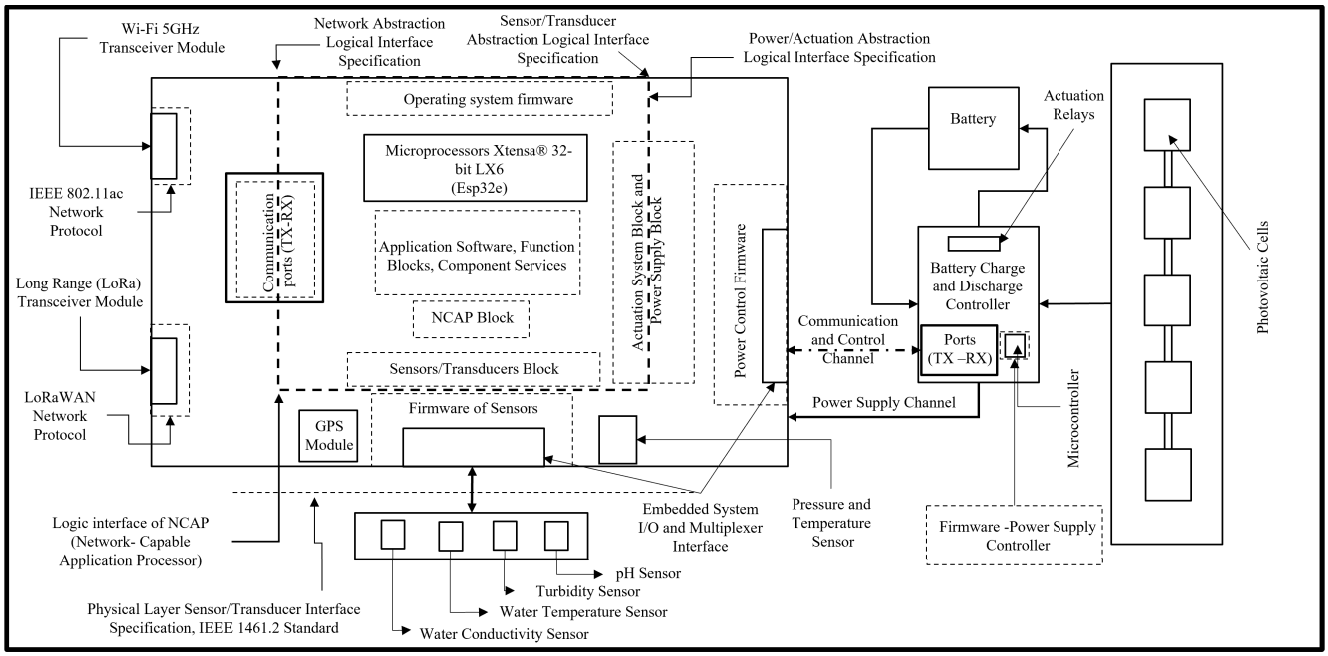

FIGURE 5. The Intelligent sensor node - the architecture of the embedded system.

to the physical part of the embedded system, as well as the structure of the system and the distributed signal acquisition network. The main components incorporated into the structure are the network capable application processor (NCAP-part of the structure that performs communications between the STIM and the network), the smart transducer interface module (STIM), and the communication interface between the sensors and microcontroller/microprocessor introducing the logical functions and online reprogramming from an integrated development environment (IDE). The software-programmable interface supports communication interfaces compatible with NCAP and STIM in the same embedded system structure, which compiles algorithms that can capture and process signals on the device itself, and enables connection with other devices through IoT techniques via the 1451.1 protocol.

The proposed embedded system structure has a subsystem that is responsible for powering the device, as shown in Figure 5. The power subsystem has an independent microcontroller to reduce the control functions in node power management. However, there is direct communication and hierarchical dependence on the microprocessor. The power subsystem is responsible for controlling battery charging and discharging and manages the power supply from the photovoltaic panels to the embedded system. However, all decision-making and response instructions are determined by the central controller.

Internal and external communications are conducted by the TX-RX ports (the ESP32 chip has more than one pair of communication ports) and embedded Wi-Fi 2.4 and 5 GHz in the chip itself. In the proposed system, the microcontroller communicates through the TX1-RX1 ports with the power subsystem, and for LoRa transmission uses the traditional TX-RX ports, as shown in Figure 5.

The set of sensors shown in Figure 5 is divided into two classes, liquid surface contacts and internal sensors. Liquid contact sensors are responsible for carrying out measurements and observations at the water level. The sensors used in the application are: DS18b20 temperature sensor, TDS V1.0 module conductivity of liquids, for pH measurement is used the ph4502C sensor and for turbidity the ST100. The GPS module is located inside and is responsible for locating the static node and determining whether the node is active or has been displaced by some external factor. Another internal sensor, the BMP180 sensor, measures pressure at sea level and ambient temperature. The transceiver chosen is the RF module wireless LoRa (Long Range) 433 MHz radio frequency transmitter and receiver, featuring low power consumption and long-distance communication.

C. SENSOR NODE PHYSICAL STRUCTURE

The proposed structure is based on studies and bibliographical research, access to materials and contact with researchers in the field of Fisheries Engineering and Oceanography. Modeling and testing of sensor node structure are performed in software from Autodesk Inventor. In Figure 6, you can see the model simulated in a computational environment.

In Figure 6, with the physical structure in green against polyethylene (PE) plastic, which is used due to its physiochemical properties. PE does not melt or deteriorate in the presence of fuels, and due to its mechanical properties, it is resistant to friction, salinity, and the effects of prolonged sun exposure. For flotation a Class 1 Circular Lifebuoy 70 cm is simulated, which has the following

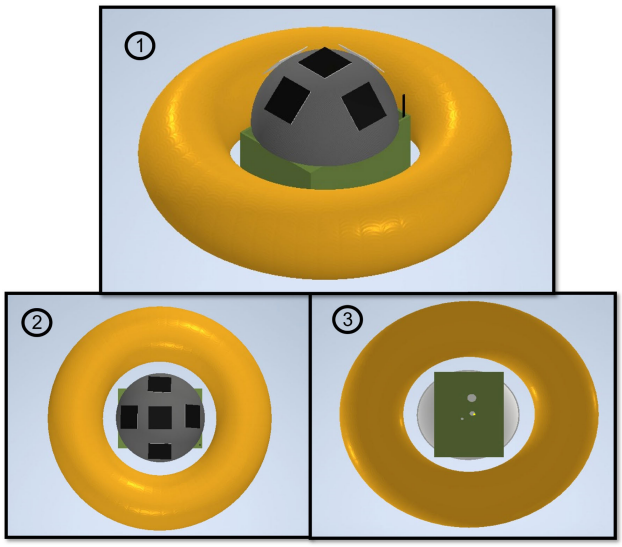

FIGURE 6. 3D Modeling of the sensor node for aquatic environments.

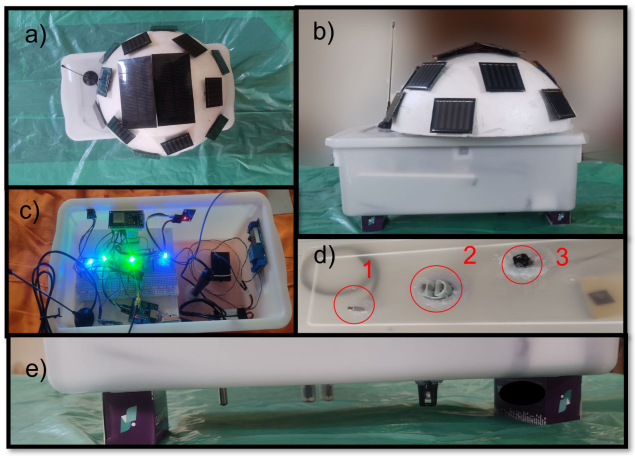

FIGURE 7. Physical structure of the sensor node - Prototype V1.

characteristics - Diameter: 70 cm - Weight: 2.5 kg. For open sea vessels and platforms, the minimum breaking load is 500 kg. Made of cast polyethylene with UV protection and internal filling of expanded polyurethane. Material resistant to fungus, seawater, fresh water, oil and its derivatives. Polypropylene cable of 10 mm braided into the float, fixed at four points. Mini photovoltaic panels are used for power supply, to recharge the batteries, distributed under a semi-sphere of 180 degree.

Figure 7 shows the designed physical structure of the proposed sensor node, first prototype, for the sensing experiments. Figure 7 is divided into 5 parts, each of which refers to a perspective of the prototype called "V1".

In Figure 7, (a) and (b) represent the mini photovoltaic cells responsible for supplying the sensor node's energy supply, alongside the communication antenna. 7 (c) presents the internal part of the embedded system, observing the microcontroller, internal sensors and battery charge and discharge control. 7 (d) and (e) show the liquid surface contact sensors: (1) the temperature sensor, (2) the turbidity sensor, and (3) the pH sensor.

TABLE 1. Seawater and fresh water pH and turbidity sensor node measurements.

Measurements	Water type			
	Seawater		Fresh water	
	pH	Turbidity (NTU)	*pH*	Turbidity (NTU)
2	7.08	2893	5.52	2486
5	7.11	2885	6.10	2905
7	7.04	2895	6.17	2397
8	7.01	2890	6.11	2348
9	7.09	2881	6.13	2406
16	7.76	2898	6.11	2460
18	7.74	2714	6.06	2456

V. DETECTION AND CLASSIFICATION TESTS

The description of the procedure and the results of the detection and classification tests for an indoor assessment of the sensor node are presented in this section. The tests measured the pH and turbidity of seawater and fresh water. The results of experiments with gasoline and diesel oil are presented to evaluate the algorithms' performance in detection and classification.

In the tests conducted at the Embedded Systems and Intelligent Control Laboratory (LabSECI) at the Federal University of Maranhão (UFMA), it is possible to detect and classify the fuel present in the water. Water contact sensors are used for testing pH, Turbidity, and Temperature. The observed variables are liquid temperature, pH, and the turbidity of the liquid given in NTU (Nephelometric Turbidity Unit, which means that the instrument is measuring the scattered light of the sample at an angle of 90 degree in relation to the incident light) in addition to the parameters of internal components of the embedded system, such as pressure at sea level, liquid temperature, internal temperature, and GPS location coordinates.

A. MEASUREMENT TESTS FOR PH AND TURBIDITY WITH SEAWATER AND FRESH WATER

The first tests and calibration of the sensors are conducted in the laboratory. In these first tests, the pH and turbidity levels of fresh water and seawater, collected at Ponta d'Areia beach in São Marcos Bay, São Luís, Maranhão, Brazil, are measured.

Table 1 presents the results of the first test of the pH level (hydrogen potential) of the analyzed water samples. pH measures how acidic or alkaline water is, with 7 being neutral. Values above 7 indicate an increase in the degree of alkalinity, and below 7 (up to 0), an increase in the degree of acidity of the medium. Some substances have their toxic effects attenuated or amplified at extreme pHs, such as those present in chemical residues.

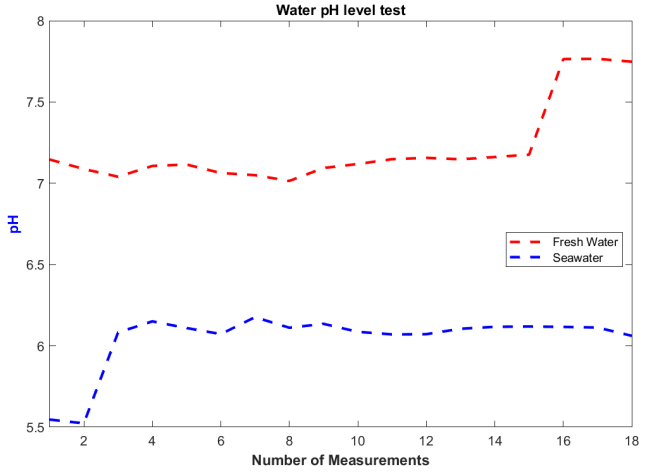

FIGURE 8. Measurement with sensor node - pH of fresh water and seawater comparison.

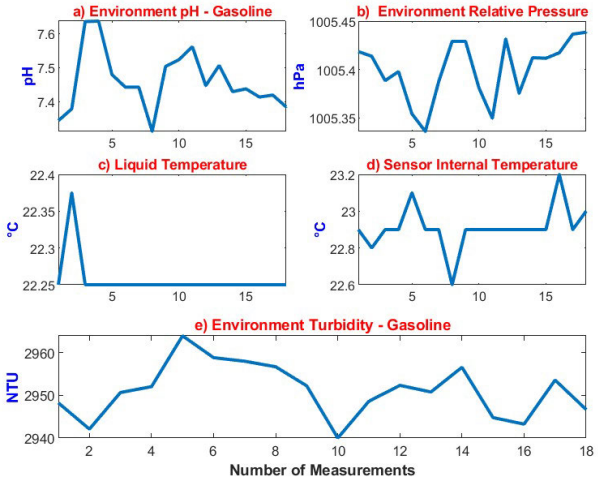

FIGURE 9. Measurements with sensor node and classification of gasoline with seawater.

The ph4502 sensor, 2000 ml of seawater, and 18 measurements at 30 s intervals are used in the first experiments. The results of seawater and fresh water pH measurements are shown in Figure 8. In Table 1, it is observed that the pH varied between 7.64 and 7.8. These variations occurred due to sediments dissolved in the water, caused by the mouths of two rivers in São Marcos Bay. The average pH of São Luís beaches is between 7 to 8.

The freshwater pH measurement test was performed with 2000 ml, and the freshwater pH level measurements ranged between 6.06 and 6.18, stabilizing the measurement at 6.13. Following the pattern of 18 measurements with 30 s intervals, the sensor took a few minutes to calibrate due to minimal variation.

Knowing that acid solutions have a pH that ranges from 0 to 7, it can be seen that fresh water has an acidic character, and seawater has a character tending more toward neutral.

The calibration of the ST100 sensor is initially performed for the measurement of turbidity. Turbidity measures how difficult it is for a beam of light to pass through a certain amount of water, giving it a cloudy appearance. This measurement is performed with a turbidimeter or nephelometer, which compares the scattering of a light beam passing through the sample with that of a beam of equal intensity passing through a standard suspension. The greater the scattering, the greater the turbidity. The table turbidimeter on the side can measure turbidity in three scales: 0 - 20, 0 - 200, and 0 - 1.000 NTU, and in the 0 - 20 scale, the resolution is 0.01 NTU. The main causes of water turbidity are the presence of solid matter in suspension (silt, clay, silica, colloids), finely divided organic and inorganic matter, microscopic organisms, and algae. In addition to reducing sunlight penetration into the water column, turbidity inhibits algae photosynthesis. Because of the sensor's sensitivity, the graphs were plotted using a 1000 times scale.

In the measurements of the fresh water samples shown in Table 1, two amplitudes can be seen between measurements 8 and 12. This noise occurs because the ST100 sensor is an infrared optical sensor that is very sensitive to large light sources and interferes with some measurements. In addition to fresh water having greater transparency than seawater (the number of particulate matter is minimal), thus having a greater incidence of light, the container where fresh water was stored is transparent, suffering more from external noise from lamps, sunlight, and computer screens.

B. GASOLINE EXPERIMENTS

The second stage of the measurements is conducted with all the sensors already embedded in the node prototype. To perform the gasoline tests shown in Figure 9, 250 ml of seawater and 100 ml of regular gasoline are used.

In Figure 9, presents the results of detection and classification. To perform the classification, it is assumed that the gasoline's turbidity is between 2.36 and 2.42 NTU and its pH is between 6.5, and 7, at ambient temperatures ranging from 18 to 40°C. The behavior of the turbidity indexes, generated from the measurements of the gasoline press on the seawater layer contained in the flask, is observed to vary between 2.948 and 2.964 NTU. The peaks of variations in the measurements were due to a large number of sediments present in the seawater sample. The pH measurements of gasoline with seawater shown in the table vary between 7.31 and 7.65, becoming stable at a value of 7.39. During the pH test, there were no problems with its measurement.

The Figure 9 represent the set of 18 measurements of a) pH of the environment with gasoline, b) relative pressure of the environment, c) liquid temperature, d) internal temperature of the sensor, and e) turbidity of the environment.

According to Figure 9, there are no significant variations in liquid temperature measurement, as it is a controlled environment where the liquid temperature remains almost the same as the ambient temperature (laboratory), with a difference of 2°C in the liquid. The internal temperature of

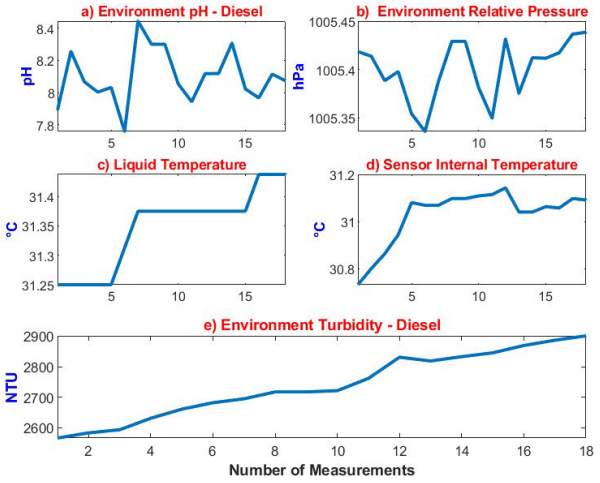

FIGURE 10. Measurements with sensor node and classification of diesel oil in seawater.

the sensor node shows a greater variation due to the presence of electronic components and internal heat dissipation, but this variation is only 0.4 degrees.

C. EXPERIMENTS - DIRECT MEASUREMENTS OF H_2O SEAWATER AND DIESEL

A qualitative view of the behavior of the measured variables of seawater with diesel oil is presented using the graphs in Figure 10. The graphs presented are from direct measurements of the pH, pressure, temperatures, and turbidity sensors. Moreover, each graph is plotted for a set of 18 measurements taken by the proposed and implemented sensor node, as presented in Figure 7, for the detection experiments. The samples of seawater mixed with diesel has a volume of 250 ml of seawater and a volume of 120 ml of diesel oil.

The following parameters are considered to detect and classify diesel: turbidity between 2.28 (2280) and 2.35 (2399) NTU, and pH of 5.8 to 6.5 under ambient conditions. Considering these values and pressure at sea level, it is possible to classify diesel.

An analysis of the sensor's ability to perform measurements is presented in Figure 10. In the graph a) of Figure 10, the pH measurement results of the environment with diesel oil are presented, with pH values ranging between 7.9 and 8.4. The obtained values are different from their natural state (before being contaminated/coming into contact with water), which occurs due to the absorption of water molecules by the diesel and the penetration of light into the environment.

Regarding the measurements related to internal pressure presented in Figure 10, the pressure measurements are relative to sea level. The relative pressure remains at 1005.48 hPa in Figure 10. According to the Government Portal, the sea level pressure of São Luís - Maranhão is, on average, 1014 hPa. This difference between the average and the measured value is due to the precision error of the sensor, which is 5%, and also because the relative pressure takes into account the ambient temperature - the higher the temperature, the lower the calculated relative pressure.

In graphics c) and d) of Figure 10, the temperature variations of the liquid and the internal part of the sensor are shown. Variations are minimal as the experiment was conducted in a controlled environment. When performing tests at sea, these circumstances tend to change since the temperature of seawater and fuel has different thermal conductivities, influenced by exposure to sunlight and marine currents.

In graph e) of Figure 10, ambient turbidity measured in the test with diesel between 2.55(2550) to 2.95(2950) NTU are presented. As with gasoline turbidity in Figure 9, the values obtained from the measurements suffer disturbances caused by an external light source. However, it does not change the final classification result.

TABLE 2. Detection and classification of mlp neural network - for gasoline and diesel fuels.

MLP Classifier - Parameters and Metrics			
Test	Accuracy(%)	Epoch	Mean Error
1	83	100	$8 \cdot 10^{-5}$

D. DETECTION AND CLASSIFICATION VIA NEURAL NETWORK FOR FUELS

The classification step was performed through an artificial neural network embedded in the device. The Table 2 presents the parameters and metrics of the multilayer neural network tests for the detection and classification of gasoline and diesel. To perform the classification, turbidity, pH, natural water temperature, and temperature of the main types of gasoline and diesel found on the market are considered, and the "natural" pH of seawater is also considered. Seawater samples are collected at Ponta d'Areia beach in São Luís-MA. In this way, it is possible to develop a classifier based on an MLP neural network with 4 neurons in the input layer and two hidden layers, each with 3 neurons, with a backpropagation training algorithm. Supervised training is performed with a set of size 1984×4 samples. The learning rate is $\eta = 0.0001$, and the initial weights of the network are random variables given by a Gaussian distribution with mean zero and variance equal to 1. It is worth noting that the set of tests is performed with the 100 measurements for each fuel present in seawater.

For a better evaluation of the model, a confusion matrix was developed, as presented in Figure 11. The purpose of the confusion matrix is to aid in the evaluation of machine learning models for classification [8], [13].

According to the obtained results, it was possible to correctly classify that 54 samples contained fuel presence and predicted that 29 samples did not contain fuel, only water. It misclassified 7 samples as fuel and 10 as water. Analyzing the table allowed for an accuracy of 83%, as it correctly predicted 83 out of 100 cases. Sensitivity was 88%, representing the probability of detecting the presence

Confusion Matrix - Classification of the presence of Fuel in water

		Positive	Negative	
Classes	Presence of Fuel	True Positive 54	False Negative 7	Sensitivity 0.88
	Water without Fuel	False Positive 10	True Negative 29	Specificity 0.74
	f-Score	Precision	False alarm rate	Accuracy
	0.86	0.84	0.26	0.83

FIGURE 11. MLP classifier performance evaluation via confusion matrix.

of fuel in the water. Specificity was 74%, representing the probability of correctly identifying the absence of an event, given that it's absent. The false alarm rate was 26% (approximately 1/4 of the estimates), which is the probability of misclassifying whether fuel presence is true or false. Taking into account that the highest possible value of an F-score, close to 1, indicates satisfactory precision and sensitivity, and the lowest possible value is 0; if the precision or sensitivity is zero, the rating is unsatisfactory/poor. Consequently, due to the fact that the F-score metric value reached 86%, it is said that the proposed MLP classifier presented good precision and sensitivity.

E. ANALYSIS AND COMMENTS OF THE IMPLEMENTATION AND TESTS

The results of the experiments are satisfactory, considering the difficulty in differentiating between fuels. To improve the sensor, one of the main parameters to be observed is the electrical conductivity of the liquid. The range of fuels and pollutants that can be detected and classified can be expanded with this implementation in the next generation of sensors.

During the tests, difficulties arose regarding the conditions of the fuels due to the odor and risk of sample contamination, as well as the risk of damaging the sensors used in the tests due to the chemical structure of the fuels employed. Direct and indirect measurements were consistent with the specifications, and it was possible to achieve the objectives of classifying and detecting the presence of fuel in water. It was also possible to embed a machine learning-based algorithm that performed the classification of diesel and gasoline. One of the expected contributions was in the indoor classification of the compound present in the water.

The node's power consumption relationship is based on its components and their usage over a period of time. Therefore, in Table 3, we present the values (Ultra-Low-Power, No signal transmission operations, only internal processing, and with signal transmission via Bluetooth and Wi-Fi according to the datasheet), as well as the tests conducted comparing theoretical consumption with real consumption at an ambient temperature ranging from 26°C to 32°C. The microcontroller used was the ESP32 NodeMcu - DevKit v1, featuring a CPU: Xtensa®Dual-Core 32-bit LX6 with 448 kBytes of ROM memory, 520 kBytes of RAM, 4 MB of flash memory, and a maximum clock of 240 MHz.

The sensor node's consumption for the real test was carried out with internal processing (only logical functions and the MLP algorithm functioning internally), resulting in a

TABLE 3. Processing system consumption μC ESP32 at 3.3 V.

Manufacturer Consumption			Consumption in real tests	
Modo: Ultra Low-Power	Bluetooth On	Wi-Fi Transmission	Internal Processing	Wi-Fi Transmission
10 μA 33 μW	75 mA 247 mW	240 mA 700 mW	75 mA 247 mW	150 mA 495 mW

TABLE 4. Power consumption of the sensor nodes.

Sensor	Measurement	Power Consuption	
		Manufacturer	Actual
ST100	Turbidity	30mA-99mW	30mA-99mW
ph4502c	pH	151mA-500mW	151mA-500mW
BMP180	Atmospheric pressure Ambient temperature	5μA - 16.5μW	5μA-16.5μW
TDS V1.0	Electric conductivity	6mA-19.8mW	6mA-19.8mW
DS18b20	Temperature Liquids	3μA- 9.9μW	3μA-9.9μW
GY-NEO6MV2	Localization	45mA-148.5mW	45mA-148.5mW

consumption of 75 mA - 247 mW. This was achieved with a sample sending rate interval of 15 s for each processed sample. The execution of signal capture and processing led to a consumption of 150 mA - 495 mW. The same sampling criteria and capture interval were used, and the signal was sent to a data storage server. In this manner, a consumption and sending test was conducted over a 15 s interval for signal transmission via Wi-Fi. It's important to note that tests using the Ultra-Low-Power mode were not performed; however, the next step will involve the implementation of the new consumption mode.

Comparative consumption tests for the node's sensors were conducted and are presented in Table 4. The table displays the observed magnitude and the consumption of each sensor according to the manufacturer's specifications. It's worth noting that the table doesn't consider losses and gains related to thermal phenomena.

The tests results presented in Table 4 showed that the sensors exhibited behavior consistent with what is described in the datasheet. The only component that displayed behavior different from what was specified was the LoRa radio frequency technology. According to the manufacturer, it was expected to have a consumption of 120 mA - 100 mW, but in the communication tests involving data transmission and reception, the consumption was around 400mW (rounded value).

The components with the highest consumption were the 433 MHz LoRa communication module, which according to its manufacturer has a consumption of 120 mA - 100 mW for broadcast, but in the applied tests it was possible to reach a consumption of 120 mA - 396 mW, and another component with higher consumption was the pH sensor due to the complexity and robustness of its secondary circuit. This circuit not only measures the pH, but also evaluates the temperature of the liquid. Total consumption was approximately 1120 mW to 1200 mW, with standby consumption of only 50 mW, which is passive and receives information from the base station. All tests in operation were

applied a voltage of 3.3 V for all components of the embedded system.

For the next tests and experiments, a new watchdog will be integrated and tested to monitor failures in readings and communications. This, combined with a low-power algorithm, will manage energy expenses more efficiently.

The work presents innovative concepts and structure, which contribute to a mathematical model of measurements based on set theory, internal processing and energy consumption. Compared to [9], [11],and [23], the methodology developed in this work uses contact sensors, analyzing water quality indices and classifying them online, avoiding common problems such as: image analysis (shading, photo analysis problems, large database), as well as the energy factor if drones are used (very high energy costs, even covering a large area is a costly task from both an energy and financial point of view).

One of the contributions is the implementation of an artificial neural network that performs detection and classification directly in the environment, facilitating more efficient detection when compared to [7], which depends directly on environmental conditions. The proposed system is capable of operating 24 hours a day, since it has a flexible setup and also uses energy harvesting techniques, extending the useful life of the node. Compared to [7], [11], [21], [23], [30], and [32], another positive point is the internal processing technology and signal transmission over long distances. Finally, compared to sensing techniques that are based on images, this work contributes to the effective detection and classification of oil-based pollutants, since current techniques depend heavily on weather conditions, wind, among other environmental points, and are very costly.

The aim of this work was to develop an architecture for an intelligent sensor node, featuring a low-cost hardware structure, a mathematical structure for observing environmental variables, energy harvesting with a charge and discharge controller that aims to balance so as not to saturate the battery, and an MLP-type artificial neural network that promotes the detection and classification of indices based on direct and indirect measurements through contact sensors. Another differentiator is that the communication system can send the signal in real time over a distance of up to 30 km, and all this with low power consumption and easy assembly and prototyping. It can be attached to a variety of structures, buoys, boats, ROVs and drones, allowing for greater versatility of applications, whether at sea, in rivers or lakes.

VI. CONCLUSION

A methodology for the conception and design of WSN sensor nodes based on embedded systems, MLP neural networks, and IoT approaches was presented in this article. The proposed methodology was applied for the detection of pollutants in aquatic environments and it was found that the proposed and developed static sensor node presented satisfactory results in identifying and classifying the presence of chemical compounds in a controlled environment.

The classification was conducted, with the measurement and detection of the process having increased indices of observed variables. As a result, the distributed processing in the microcontroller cores contributed to a lower computational effort, resulting in lower energy consumption and increasing the node survival time. Notably the use of distributed processing within the node's processor cores influenced a better detection response and classification of the embedded MLP artificial neural network algorithm.

REFERENCES

[1] K. S. Adu-Manu, N. Adam, C. Tapparello, H. Ayatollahi, and W. Heinzelman, "Energy-harvesting wireless sensor networks (EH-WSNs): A review," *ACM Trans. Sensor Netw.*, vol. 14, no. 2, pp. 1–50, Apr. 2018.

[2] Z. Asif, Z. Chen, C. An, and J. Dong, "Environmental impacts and challenges associated with oil spills on shorelines," *J. Mar. Sci. Eng.*, vol. 10, no. 6, p. 762, May 2022.

[3] A.-L. Balogun, S. T. Yekeen, B. Pradhan, and K. B. W. Yusof, "Oil spill trajectory modelling and environmental vulnerability mapping using GNOME model and GIS," *Environ. Pollut.*, vol. 268, Jan. 2021, Art. no. 115812.

[4] A. M. Bernabeu, M. Plaza-Morlote, D. Rey, M. Almeida, A. Dias, and A. P. Mucha, "Improving the preparedness against an oil spill: Evaluation of the influence of environmental parameters on the operability of unmanned vehicles," *Mar. Pollut. Bull.*, vol. 172, Nov. 2021, Art. no. 112791.

[5] M. Bhuyan, *Intelligent Instrumentation: Principles and Applications*. Boca Raton, FL, USA: CRC Press, 2013.

[6] C. M. Bishop, *Pattern Recognition and Machine Learning* (Information Science and Statistics), 1st ed. Springer, 2006.

[7] H. Denkilkian, A. Koulakezian, R. Ohannessian, M. S. Chalfoun, M. K. W. Joujou, A. Chehab, and I. H. Elhajj, "Wireless sensor for continuous real-time oil spill thickness and location measurement," *IEEE Trans. Instrum. Meas.*, vol. 58, no. 12, pp. 4001–4011, Dec. 2009.

[8] R. C. Eberhart and Y. Shi, *Computational Intelligence: Concepts to Implementations*, 1st ed. San Mateo, CA, USA: Morgan Kaufmann, 2007.

[9] M. Fingas and C. Brown, "A review of oil spill remote sensing," *Sensors*, vol. 18, no. 2, p. 91, Dec. 2017.

[10] D. D. Gajski, G. S. S. Abdi, and A. Gerstlauer, *Embedded System Design: Modeling, Synthesis and Verification*, 1st ed. Springer, 2009.

[11] O. Garcia-Pineda, G. Staples, C. E. Jones, C. Hu, B. Holt, V. Kourafalou, G. Graettinger, L. DiPinto, E. Ramirez, D. Streett, J. Cho, G. A. Swayze, S. Sun, D. Garcia, and F. Haces-Garcia, "Classification of oil spill by thicknesses using multiple remote sensors," *Remote Sens. Environ.*, vol. 236, Jan. 2020, Art. no. 111421.

[12] I. Goodfellow, Y. Bengio, and A. Courville, *Deep Learning* (Adaptive Computation and Machine Learning Series). Cambridge, MA, USA: MIT Press, 2016.

[13] A. Géron, *Hands on Machine Learning With Scikit Learn Keras and TensorFlow*, 2nd ed. O'Reilly Media, 2019.

[14] L. Haulin, "A state-based method to model and analyze the power consumption of embedded systems," Tech. Rep., 2018.

[15] R. Hidalgo-Leon, J. Urquizo, C. E. Silva, J. Silva-Leon, J. Wu, P. Singh, and G. Soriano, "Powering nodes of wireless sensor networks with energy harvesters for intelligent buildings: A review," *Energy Rep.*, vol. 8, pp. 3809–3826, Nov. 2022.

[16] P. Keramea, K. Spanoudaki, G. Zodiatis, G. Gikas, and G. Sylaios, "Oil spill modeling: A critical review on current trends, perspectives, and challenges," *J. Mar. Sci. Eng.*, vol. 9, no. 2, p. 181, Feb. 2021.

[17] C. Koulamas and M. Lazarescu, "Real-time embedded systems: Present and future," *Electronics*, vol. 7, no. 9, p. 205, Sep. 2018.

[18] E. A. Lee and S. A. Seshia, *Introduction to Embedded Systems: A Cyber-Physical Systems Approach*, 2nd ed. Cambridge, MA, USA: MIT Press, 2017.

[19] I. M. M. El Emary and S. Ramakrishnan, *Wireless Sensor Networks: From Theory to Applications*, 2013.

[20] P. Marwedel, *Embedded System Design: Embedded Systems Foundations of Cyber-Physical Systems, and the Internet of Things*, 4th ed. Springer, 2021.

[21] Q. Mascret, G. Gagnon-Turcotte, M. Bielmann, C. L. Fall, L. J. Bouyer, and B. Gosselin, "A wearable sensor network with embedded machine learning for real-time motion analysis and complex posture detection," *IEEE Sensors J.*, vol. 22, no. 8, pp. 7868–7876, Apr. 2022.
[22] S. C. Mukhopadhyay, S. K. S. Tyagi, N. K. Suryadevara, V. Piuri, F. Scotti, and S. Zeadally, "Artificial intelligence-based sensors for next generation IoT applications: A review," *IEEE Sensors J.*, vol. 21, no. 22, pp. 24920–24932, Nov. 2021.
[23] P. Odonkor, Z. Ball, and S. Chowdhury, "Distributed operation of collaborating unmanned aerial vehicles for time-sensitive oil spill mapping," *Swarm Evol. Comput.*, vol. 46, pp. 52–68, May 2019.
[24] A. D. Pimentel, "Exploring exploration: A tutorial introduction to embedded systems design space exploration," *IEEE Des. Test.*, vol. 34, no. 1, pp. 77–90, Feb. 2017.
[25] S. S. Saha, S. S. Sandha, and M. Srivastava, "Machine learning for microcontroller-class hardware: A review," *IEEE Sensors J.*, vol. 22, no. 22, pp. 21362–21390, Nov. 2022.
[26] R. Sanchez-Iborra and A. F. Skarmeta, "TinyML-enabled frugal smart objects: Challenges and opportunities," *IEEE Circuits Syst. Mag.*, vol. 20, no. 3, pp. 4–18, 3rd Quart., 2020.
[27] R. R. Selmic, V. V. Phoha, and A. Serwadda, *Wireless Sensor Networks: Security, Coverage, and Localization*, 2016.
[28] K. Sohraby, D. Minolia, and T. Znati, *Wireless Sensor Networks: Technology, Protocols, and Applications*, 2007.
[29] S. Soloman, *Sensors Handbook*, 2nd ed., 2009.
[30] G. Tabella, N. Paltrinieri, V. Cozzani, and P. S. Rossi, "Wireless sensor networks for detection and localization of subsea oil leakages," *IEEE Sensors J.*, vol. 21, no. 9, pp. 10890–10904, May 2021.
[31] Y. K. Tan, *Energy Harvesting Autonomous Sensor Systems: Design, Analysis, and Practical Implementation*. Boca Raton, FL, USA: CRC Press, 2013.
[32] S. T. Yekeen and A.-L. Balogun, "Advances in remote sensing technology, machine learning and deep learning for marine oil spill detection, prediction and vulnerability assessment," *Remote Sens.*, vol. 12, no. 20, p. 3416, Oct. 2020.
[33] X. Wang, R. Hoseinnezhad, A. K. Gostar, T. Rathnayake, B. Xu, and A. Bab-Hadiashar, "Multi-sensor control for multi-object Bayes filters," *Signal Process.*, vol. 142, pp. 260–270, Jan. 2018.
[34] M. Wolf, *Computers as Components: Principles of Embedded Computing System Design* (The Morgan Kaufmann Series in Computer Architecture and Design), 3rd ed. Amsterdam, The Netherlands: Elsevier, 2012.

YAN FERREIRA DA SILVA received the degree in control and automation engineering from Faculdade Pitagoras de São Luís, in 2018, and the master's degree in electrical engineering from Universidade Federal do Maranhão, in 2020, where he is currently pursuing the Ph.D. degree in electrical engineering. He is also pursuing the Ph.D. degree with the Human Resources Training (PRH), Universidade Federal do Maranhão. His research interests include computational intelligence, machine learning, wireless sensor networks, intelligent sensors, robotics, and industrial process automation.

RAIMUNDO CARLOS SILVÉRIO FREIRE (Member, IEEE) was born in Poco de Pedra, Rio Grande do Norte, Brazil, in October 1955. He received the B.S. degree in electrical engineering from Universidade Federal do Maranhão, Brazil, in 1980, the M.S. degree in electrical engineering from the Federal University of Paraíba, Campina Grande, Brazil, in 1982, and the Ph.D. degree in electronics, automation, and measurements from the National Polytechnic Institute of Lorraine, Nancy, France, in 1988. He was an Electrical Engineer with Maranhão Educational Television, from 1980 to 1983. He was a Professor of electrical engineering with Universidade Federal do Maranhão, from 1982 to 1985. From 1989 to 2002, he was a Full Professor with the Federal University of Paraíba. Since 2002, he has been with the Electrical Engineering Department, Federal University of Campina Grande. His research interests include electronic instrumentation, microelectronics, integrated circuit design, A/D and D/A converters, RFID and SAW, and sensors.

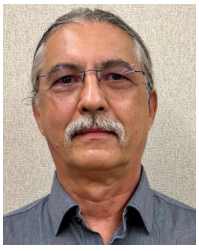

JOÃO VIANA DA FONSECA NETO (Member, IEEE) received the bachelor's and master's degrees in electrical engineering from the Federal University of Paraíba, in 1982 and 1986, respectively, and the Ph.D. degree in electrical engineering from the State University of Campinas, in 2000. He is currently a Full Professor with Universidade Federal do Maranhão (UFMA). His research interests include computational intelligence, multi-agent systems, machine learning, sensors networks, optimal control, and evolutionary computation and fuzzy.